Spatially coherent late-Holocene Antarctic Peninsula surface air temperature variability

SUPPLEMENTAL INFORMATION

Moss bank core collection and sampling

Cores were collected in January 2012 (Elephant Island; 61.111°S, 54.824°W, Barrientos Island; 62.408°S, 59.753°W, Norsel Point; 64.759°S, 64.084°W) and January 2013 (Green Island; 65.322°S, 64.151°W, Leonie Island; 67.602°S, 68.343°W). Figure S1 shows a selection of sample locations, characteristics and coring approaches. Monoliths were carefully removed from non-permafrost near-surface sediments. Deeper cores were sampled using a permafrost corer (Nornberg et al., 2004) until the base of the moss bank was reached. All cores were stored at -20°C.

Chronology and mass accumulation rates

All ^{14}C dates were measured on pure moss fragments and ^{210}Pb activity was measured on bulk samples. Age-depth models for continuous cores were developed from conventional and post-bomb ^{14}C and alpha-spectrometry ^{210}Pb (Figure S2). Raw ^{14}C dates and ^{210}Pb ages derived from a constant rate of supply model (Appleby and Oldfield, 1978) were entered into the R package 'clam' (Blaauw, 2010) to develop smooth spline models using the minimum smoothing value (lower values resulting in more flexible models) at which age reversals did not occur in the majority of model iterations. All other settings were default. Mass accumulation rates (g DM cm^{-2} yr^{-1}) were calculated using the depth, modelled ages and bulk density values for contiguous samples; bulk density (g cm^{-3}) was calculated by freeze drying samples of known volume. For ELE1 and ELE2, a hiatus was used in the age-depth model to

reflect the reported ages and stratigraphic context of the core. Details of all ^{14}C and ^{210}Pb dates and age-depth models are given in Tables S1 and S2 and age depth models are illustrated in Fig. S2.

All of our records suggested coherent age-depth models, although two moss banks have a hiatus (ELE1 and ELE2, Fig S1A and B). Whilst physical processes can affect moss bank growth dynamics at the edges (Fenton, 1982), the vertical accumulation patterns from our cores suggest that this does not affect the central moss bank areas.

Carbon stable isotopes

Cellulose was extracted from moss samples using a standard protocol (Loader et al., 1997). For $\delta^{13}C$ analysis, 1 mg samples of freeze-dried α-cellulose were transferred to tin capsules and measured at the NERC Isotope Geoscience Laboratory (British Geological Survey) by combustion in a furnace connected on-line to a dual inlet isotope ratio mass spectrometer. Isotope ratios ($^{13}C/^{12}C$) were referenced to the VPDB scale using within-run standards. Raw $\delta^{13}C$ values were converted to carbon isotopic discrimination ($\Delta^{13}C$) by reference to age depth models and records of global atmospheric $\delta^{13}C$ from Antarctica (Schneider and Steig, 2008). Cellulose $\Delta^{13}C$ represents a proxy for seasonal photosynthetic conditions (Royles et al., 2012; Seibt et al., 2008), with high discrimination values reflecting optimal hydration for maximum assimilation rates (Bramley-Alves et al., 2015).

Testate amoeba analysis

Testate amoebae were used as a proxy for microbial productivity (Royles et al., 2013). Samples were prepared according to standard methodologies (Booth, 2010), with the size fraction between 300 and 15 μm retained for microscopic analysis. Tests were counted and volumetric concentration values (tests cm^{-3}) were calculated by the addition of an exotic

spore marker, with concentration per unit surface area over time (tests cm^{-2} yr^{-1}) calculated from the age depth relationship. Minimum counts of 25 individuals were accepted for statistical analysis due to extremely low concentration in some samples.

Testate amoebae feed on bacteria and fine detritus and potentially other smaller protists. They are therefore partly dependent on the microbial community, which is in turn dependent on a complex set of variables including availability of plant material, temperature and moisture. However, the over-riding driver of microbial activity in moss communities is likely to be temperature, just as it is in soils, with availability of free water being the most common limiting factor during periods of freezing.

Correlation of temperature data with proxies

To test the relationship between the proxy data and temperature, we correlated the testate amoebae productivity and mass accumulation rate from Green Island with annual and summer temperature from Vernadsky station (Table S1). This site was selected as it is the only location where there is a long instrumental temperature record (1951-present) sufficiently close to the available moss bank records. Temperature data were derived from mean monthly data, with summer temperatures calculated as the average of December, January and February. Daily data were unavailable so we could not calculate growing degree days as a measure of growing season length. The age of each sample used was the median age estimate from the age-depth models. Combined ^{210}Pb and ^{14}C dating generates precise age estimates and dating 95% uncertainty varies between 6 and <1 years for the period since 1951, generally with uncertainty reducing from 1951 to present. Correlation coefficients were calculated for all individual samples using their closest matched year of accumulation and for five year binned data, partly to allow for the dating uncertainty and partly to allow for the fact some samples spanned multiple years.

Data compilation

Regional proxy temperature reconstructions were generated from combining the proxy data from the core data from Elephant island and Green Island. Only accumulation rate (g DM cm^{-2} yr^{-1}) and microbial productivity (i.e. testate amoeba concentration in tests cm^{-2} yr^{-1}) data were included in the standardised, binned records used for the compilation of temperature proxy data shown in Figure 3. $\Delta^{13}C$ records were not used because the proxy is reflects a combination of temperature and moisture regimes. All sites and proxies were considered equally and no weighting of individual records was applied.

There was no common period over which all records could be standardised, so all raw proxy data were standardised over the whole length of their records to produce z-scores using the equation:

$$z = \frac{x-\mu}{\sigma}$$

Where z is the z-score (in SD units), x is the individual proxy value at any given date, μ is the mean of all values in the individual dataset and σ is the standard deviation of all values in the individual dataset.

All data (i.e. including multiple cores/proxies) from ELE and GRE independently were averaged into 100 year bins to develop two individual site records (see Figure S4). For bins with values from both ELE and GRE, a mean value for used for the final regional record. Where there were only values from one site (i.e. 1000 – 1200 cal. BP and pre-1500 cal. BP), those values were used for the final regional record. Correlation coefficients were calculated for the 100 year binned data from the ice core and compiled moss bank record.

Supplemental Figure DR1: Examples of sampled moss banks and the extraordinary depths reached in these unusual circumstances. A, B and E show moss bank Elephant Island ELE 1 with deep exposed face and coring location (core depth 279cm, location S 61° 08' 36.1'' W 54° 42' 01.4'', 188 m asl); E shows depth of core indicated by length of core rods used; C shows exposed nature of Elephant Island ELE 2 (core length 200 cm, location S 61° 08' 26.5'' W 54° 41' 49.9''); D shows location of Elephant Island ELE3 in less exposed col area (core depth 33cm, location S 61° 08' 27.5'' W 54° 42' 39.8'', 169 m asl). F, G and H show large moss bank on Green Island where cores G1 and G2 were taken; F and G show sloping nature of site; H shows close up of surface microtopography. (G1 core: depth 97cm, location S: 65° 19' 23.2" W: 064° 09'04.9", 65 m asl. G2 core: depth 66cm, location S: 65° 19' 23.8" W: 064° 09'05.6" 67 m asl.).

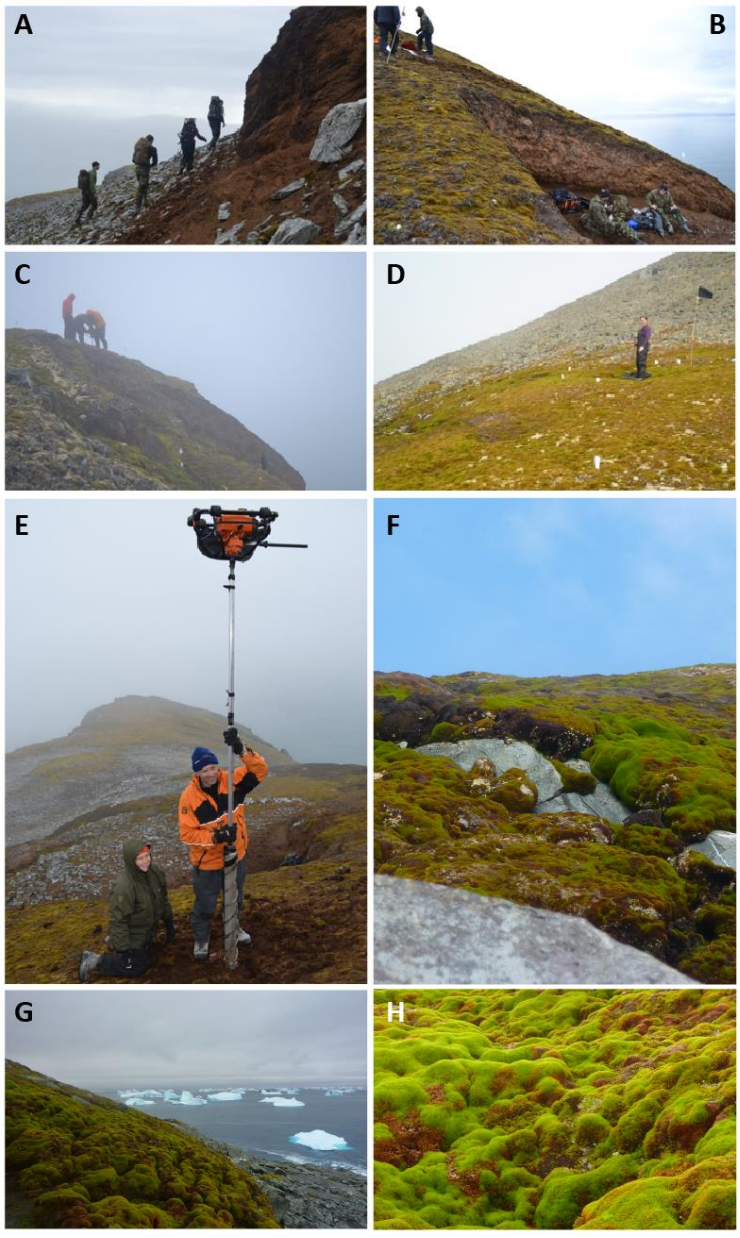

Supplemental Figure DR2: Age depth models for all sites. A = ELE1, B = ELE2, C = ELE3, D = G1, E = G2.

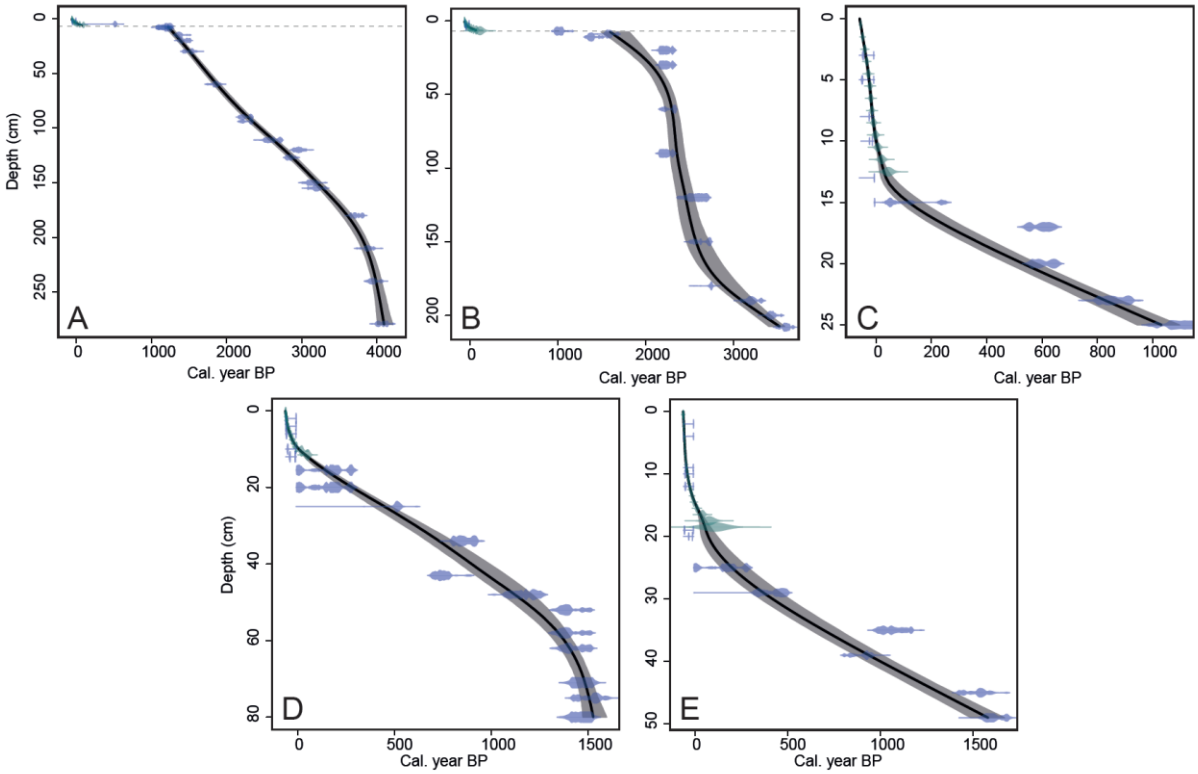

Supplemental Figure DR3: Changes in biological productivity at Elephant Island (A-C) and Green Island (D-F), shown as annual biomass accumulation (A, D), annual testate amoebae productivity (B, E), and $\Delta^{13}C$ (C, F). Note change in x axis scale for last 200 years to show higher resolution changes.

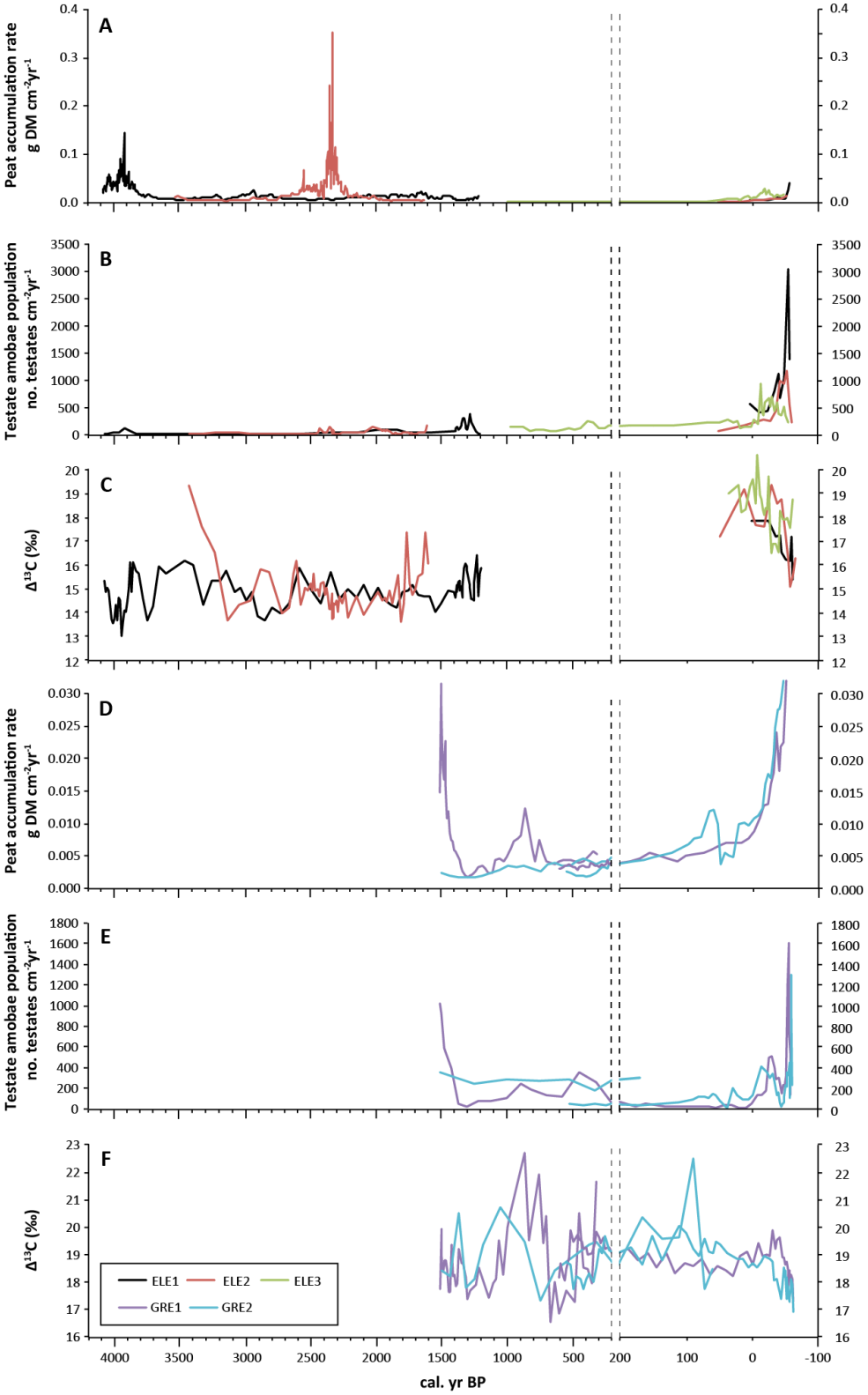

Supplemental Table DR1: Correlation coefficients (r) between the long instrumental temperature record at Vernadsky station and Green Island moss bank proxy records over the same period (cores G1 and G2). Correlations in bold $p<0.05$, except *$p=0.09$. Temperature data are either mean annual or mean summer (DJF) and correlations were calculated both from using instrumental data from the estimated individual year of each individual fossil sample and using all data in five year bin sizes.

	All data points			Five year bins		
	n	Mean annual T	Mean summer T	n	Mean annual T	Mean summer T
G1 Testate	**21**	**0.50**	**0.46**	**11**	**0.57***	0.48
G1 Accumulation rate	**21**	**0.49**	0.28	**11**	**0.61**	0.35
G2 Testate	26	0.04	0.08	13	0.24	0.07
G2 Accumulation rate	**26**	**0.47**	0.33	**13**	**0.64**	0.47

131 **Supplemental Table DR2:** Radiocarbon dates from all sites

132

Identifier	Site/core code	Sample depth (cm)	^{14}C enrichment (absolute % modern carbon, ± 1σ)	Conventional ^{14}C age (± 1σ)
SUERC-49590	ELE1	2	100.28 ± 0.44	
SUERC-46879	ELE1	3	109.41 ± 0.50	
SUERC-49591	ELE1	5		470 ± 37
SUERC-49592	ELE1	7		1269 ± 37
SUERC-49593	ELE1	8		1224 ± 35
SUERC-46880	ELE1	9		1264 ± 37
SUERC-49594	ELE1	15		1482 ± 37
SUERC-49595	ELE1	20		1532 ± 35
SUERC-43053	ELE1	30		1628 ± 38
SUERC-43056	ELE1	60		1907 ± 38
SUERC-43057	ELE1	90		2257 ± 38
SUERC-49596	ELE1	94		2279 ± 37
SUERC-49597	ELE1	111		2516 ± 37
SUERC-43058	ELE1	120		2849 ± 35
SUERC-49600	ELE1	127		2755 ± 35
SUERC-43059	ELE1	150		2967 ± 38
SUERC-49601	ELE1	155		3011 ± 36
SUERC-43060	ELE1	180		3455 ± 36
SUERC-43061	ELE1	210		3578 ± 38
SUERC-43062	ELE1	240		3636 ± 38
SUERC-43066	ELE1	279		3729 ± 38
SUERC-49603	ELE2	2	108.61 ± 0.48	
SUERC-49604	ELE2	4	114.85 ± 0.53	
SUERC-49605	ELE2	7		1114 ± 37
SUERC-49606	ELE2	9		1679 ± 35
SUERC-49607	ELE2	11		1500 ± 37
SUERC-49610	ELE2	20		2220 ± 37
SUERC-46881	ELE2	30		2223 ± 37
SUERC-46882	ELE2	60		2278 ± 37
SUERC-46885	ELE2	90		2223 ± 37
SUERC-49886	ELE2	120		2475 ± 37
SUERC-46887	ELE2	150		2542 ± 37
SUERC-46888	ELE2	180		2604 ± 37
SUERC-49611	ELE2	190		3011 ± 37
SUERC-49612	ELE2	200		3214 ± 37
SUERC-43063	ELE2	208		3350 ± 38
SUERC-54332	ELE3	3	111.56 ± 0.58	
SUERC-49613	ELE3	5	109.66 ± 0.48	
SUERC-54333	ELE3	8	138.83 ± 0.72	
SUERC-49614	ELE3	10	142.59 ± 0.63	
SUERC-54334	ELE3	13	103.10 ± 0.51	
SUERC-49616	ELE3	15		43 ± 37
SUERC-54335	ELE3	17		589 ± 39

SUERC-49617	ELE3	20		628 ± 37
SUERC-54336	ELE3	23		953 ± 39
SUERC-46889	ELE3	25		1175 ± 37
SUERC-54349	GRE1	2	104.30 ± 0.54	
SUERC-54352	GRE1	4	105.35 ± 0.54	
SUERC-49627	GRE1	6	109.62 ± 0.51	
SUERC-54353	GRE1	10	117.26 ± 0.61	
SUERC-54354	GRE1	12	106.82 ± 0.49	
SUERC-49631	GRE1	15.5		175 ± 35
SUERC-49632	GRE1	20		182 ± 35
SUERC-49633	GRE1	25		471 ± 37
SUERC-54356	GRE1	34		955 ± 37
SUERC-49634	GRE1	43		836 ± 35
SUERC-54357	GRE1	48		1234 ± 41
SUERC-49635	GRE1	52		1508 ± 35
SUERC-49636	GRE1	58		1504 ± 40
SUERC-54358	GRE1	62		1525 ± 37
SUERC-49637	GRE1	71		1579 ± 35
SUERC-49640	GRE1	75		1630 ± 41
SUERC-49641	GRE1	80		1566 ± 37
SUERC-54359	GRE2	2	104.50 ± 0.52	
SUERC-54362	GRE2	4	105.21 ± 0.54	
SUERC-49645	GRE2	9	110.48 ± 0.51	
SUERC-49642	GRE2	10	109.05 ± 0.51	
SUERC-54363	GRE2	12	109.55 ± 0.57	
SUERC-49646	GRE2	19	107.14 ± 0.50	
SUERC-49644	GRE2	20	125.18 ± 0.58	
SUERC-49647	GRE2	25		187 ± 37
SUERC-54364	GRE2	29		374 ± 41
SUERC-54365	GRE2	35		1148 ± 39
SUERC-49650	GRE2	39		1000 ± 37
SUERC-54366	GRE2	45		1634 ± 40
SUERC-49651	GRE2	49		1701 ± 37
SUERC-44335	ARD1	23		490 ± 37
SUERC-46900	ARD2	16	102.62 ± 0.47	
SUERC-44336	ARD3	20		139 ± 37
SUERC-46891	BAR3	16	103.76 ± 0.48	
UCIAMS-133561	BAR4	21		2525 ± 25
UBA-28841	LEO	25	105.46 ± 0.30	
SUERC-46897	NOR1	67		1661 ± 35
SUERC-46898	NOR2	49		42 ± 37
SUERC-46899	NOR3	44		527 ± 35

133

Supplemental Table DR3: Alpha spectrometry ^{210}Pb dating results and CRS (Constant Rate of Supply – see methods) modelled ages, with 2σ error estimates, for all sites

Site/core code	Sample depth (cm)	Pb-210 activity (Bq/kg)	± error	CRS modelled age (year AD)	± error
ELE1	0.5	55.29	3.15	2009	1
ELE1	1	61.04	3.42	2007	1
ELE1	1.5	54.00	2.89	2004	1
ELE1	2	57.19	3.25	1999	2
ELE1	2.5	61.58	3.49	1995	2
ELE1	3	81.28	4.81	1989	2
ELE1	3.5	56.68	2.97	1978	2
ELE1	4	54.19	2.94	1968	2
ELE1	4.5	36.46	1.89	1955	3
ELE1	5	31.93	1.59	1938	4
ELE1	5.5	38.97	0.92	1905	6
ELE1	6	7.74	0.61	1855	11
ELE2	0.5	44.13	2.19	2011	1
ELE2	1	59.95	3.14	2009	1
ELE2	1.5	56.44	3.22	2006	1
ELE2	2	81.07	3.44	2001	1
ELE2	2.5	66.84	3.37	1996	2
ELE2	3	66.45	3.17	1990	2
ELE2	3.5	68.12	3.32	1984	2
ELE2	4	65.76	3.11	1975	2
ELE2	4.5	59.47	3.19	1964	3
ELE2	5	55.15	3.04	1950	4
ELE2	5.5	41.35	3.43	1932	5
ELE2	6	28.79	2.57	1909	7
ELE2	6.5	18.66	1.88	1877	14
ELE2	7	10.75	1.26	1835	35
ELE3	1	34.63	1.30	2006	1
ELE3	2	34.68	1.36	1999	2
ELE3	3	27.00	1.23	1991	3
ELE3	4	27.12	1.11	1984	3
ELE3	5	23.71	1.11	1978	4
ELE3	6	21.78	1.05	1972	4
ELE3	7	19.04	0.86	1969	4
ELE3	8	21.28	1.22	1965	4
ELE3	9	22.01	1.23	1959	5
ELE3	10	21.08	1.02	1952	6
ELE3	11	21.92	1.30	1944	7
ELE3	12	23.40	1.40	1930	9
ELE3	13	22.26	1.15	1906	14
GRE1	1	14.88	0.84	2010	1
GRE1	2	14.00	0.75	2008	2

GRE1	3	19.53	1.03	2007	2
GRE1	4	20.58	1.02	2004	2
GRE1	5	34.81	1.66	1999	2
GRE1	6	29.17	1.60	1992	2
GRE1	7	23.69	1.11	1985	2
GRE1	8	21.02	1.09	1977	3
GRE1	9	22.81	1.12	1968	3
GRE1	10	20.08	0.99	1956	4
GRE1	11	24.31	1.23	1929	7
GRE1	12	10.77	0.73	1898	10
GRE2	1	11.01	0.65	2012	1
GRE2	2	23.12	0.97	2011	1
GRE2	3	21.74	0.89	2009	1
GRE2	4	22.99	1.00	2008	1
GRE2	5	22.60	1.09	2006	1
GRE2	6	14.19	0.78	2004	1
GRE2	7	25.06	1.05	2003	1
GRE2	8	26.06	1.00	2000	1
GRE2	9	27.28	1.07	1997	2
GRE2	10	33.11	1.84	1993	2
GRE2	11	28.89	1.10	1987	2
GRE2	12	28.03	1.27	1981	2
GRE2	13	23.99	1.05	1973	3
GRE2	14	17.76	0.88	1965	3
GRE2	15	21.92	1.52	1955	4
GRE2	16	20.56	1.05	1939	5
GRE2	17	19.76	0.98	1909	10
GRE2	18	6.59	0.50	1873	26
GRE2	19	6.79	0.46	1844	61

137

SUPPLEMENTAL INFORMATION REFERENCES

Appleby, P. G., and Oldfield, F., 1978, The calculation of lead-210 dates assuming a constant rate of supply of unsupported ^{210}Pb to the sediment Catena, v. 5, p. 1-8.

Blaauw, M., 2010, Methods and code for 'classical' age-modelling of radiocarbon sequences: Quaternary Geochronology, v. 5, p. 512-518.

Booth, R. K. L., M;, Charman, D.J; , 2010, Preparation and analysis of testate amoebae in peatland palaeoenvironmental studies: Mires and Peat, v. 7, p. 1-7.

Bramley-Alves, J., Wanek, W., French, K., and Robinson, S. A., 2015, Moss delta C-13: an accurate proxy for past water environments in polar regions: Global Change Biology, v. 21, p. 2454-2464.

Fenton, J. H. C., 1982, The formation of vertical edges on antarctic moss peat banks: Arctic And Alpine Research, v. 14, p. 21-26.

Loader, N. J., Robertson, I., Barker, A. C., Switsur, V. R., and Waterhouse, J. S., 1997, An improved technique for the batch processing of small wholewood samples to alpha-cellulose: Chemical Geology, v. 136, p. 313-317.

Nornberg, T., Goodsite, M. E., and Shotyk, W., 2004, An improved motorized corer and sample processing system for frozen peat: Arctic, v. 57, p. 242-246.

Royles, J., Amesbury, M. J., Convey, P., Griffiths, H., Hodgson, D. A., Leng, M. J., and Charman, D. J., 2013, Plants and soil microbes respond to recent warming on the Antarctic Peninsula: Current Biology, v. 23, p. 1702-1706.

Royles, J., Ogee, J., Wingate, L., Hodgson, D. A., Convey, P., and Griffiths, H., 2012, Carbon isotope evidence for recent climate-related enhancement of CO_2 assimilation and peat accumulation rates in Antarctica: Global Change Biology, v. 18, p. 3112-3124.

Seibt, U., Rajabi, A., Griffiths, H., and Berry, J. A., 2008, Carbon isotopes and water use efficiency: sense and sensitivity: Oecologia, v. 155, p. 441-454.

Schneider, D. P., and Steig, E. J., 2008, Ice cores record significant 1940s Antarctic warmth related to tropical climate variability: Proceedings of the National Academy of Sciences of the United States of America, v. 105, p. 12154-12158.